

# Spin Correlations in Decay Chains Involving W Bosons

---

Jennifer M. Smillie

Cavendish Laboratory, University of Cambridge,  
JJ Thomson Avenue, Cambridge CB3 0HE, U.K.  
E-mail: smillie@hep.phy.cam.ac.uk

**Abstract:** We study the extent to which spin assignments of new particles produced at the LHC can be deduced in the decay of a scalar or fermion  $C$  into a new stable (or quasi-stable) particle  $A$  through the chain  $C \rightarrow B \rightarrow A$ ;  $W \rightarrow \ell \nu$ , where  $\ell = e, \mu$ . All possible spin assignments of the particles  $A$  and  $B$  are considered in order to remain as model-independent as possible. Explicit invariant mass distributions of the quark and lepton are given for each set of spins, valid for all masses. We also construct the asymmetry between the chains with a  $W^-$  and those with a  $W^+$ . The Kullback-Leibler distance between the distributions is then calculated to give a quantitative measure of our ability to distinguish the different spin assignments.

**Keywords:** Hadronic Colliders, Beyond Standard Model, Supersymmetry  
Phenomenology, Large Extra Dimensions.

---

## Contents

1. Introduction	1
2. Spin assignments	2
3. Spin correlations	3
4. Model discrimination	9
5. Conclusions	12
A. Analytical formulae	12

---

## 1. Introduction

While the Standard Model (SM) has been remarkably successful to date, new physics is expected around the TeV scale, for example to cancel the large contributions to the Higgs mass thereby solving the Hierarchy problem. Whatever form this new physics takes, we expect to find new particles. The issue of deducing the spin of these new particles from experimental data has become increasingly important with the rise in popularity of supersymmetric (SUSY) extensions to the SM. These models assign to SM partners different spin to that of the corresponding SM particle. This is in contrast to another possible SM extension, Universal Extra Dimensions (UED) [1] where each SM partner has the same spin as its SM counterpart. There are also other possible extensions to the Standard Model where there are different spin assignments to new particles, such as new scalars in Little Higgs Models [2].

Often, studies of spin are considered in the context of a linear electron collider. However, Barr [3] (see also [4]) showed that it was possible to deduce such information at the Large Hadron Collider (LHC). He demonstrated that one could distinguish between the case where particles had SUSY spin allocations and where the particles were all effectively spinless. This work was extended in [5, 6, 7, 8, 9, 10] to demonstrate that spin studies were a useful tool to distinguish between SUSY and UED. (It was first pointed out in [11] that these two models could mimic each other.) Recently [12], the technique was extended to cover all possible spin assignments in the cascade decay of a quark partner via opposite-sign same-flavour (OSSF) leptons. This had much wider applications as it was no longer constrained to spin effects only in the Minimal Supersymmetric Standard Model (MSSM) and UED. A similar study had previously been applied in [13] to the pair production of top quark partners each decaying straight to a top and a stable particle.

These studies have concentrated on the quark partner cascade decay (or gluino decay leading to this), top partner production and Drell-Yan production of lepton pairs and their subsequent decay. Here we study the electroweak decay of a quark partner via a  $W$  boson decaying leptonically. In the MSSM, this decay chain often has a higher branching ratio than the cascade decay via a  $e_2^0$  which is more frequently studied. In [14], it is suggested that this could be the most promising channel for spin discrimination. Here, we consider all possible spin assignments so as not to constrain ourselves to a particular model. We assume that these chains have been identified, and that the masses of the particles involved are known. The spin correlations in the chain depend on the charge of the  $W$  boson, so we consider the two charge assignments separately.

In section 2, we discuss all possible spin assignments in the decay chain and the resulting matrix elements. In section 3, spin correlations are discussed in terms of the invariant mass distributions of the quark and lepton. The full analytical formulae valid for any mass spectrum are calculated. We then form an asymmetry between the chains with a  $W^-$  and the chains with a  $W^+$ . These distributions are plotted and discussed. In section 4, we quantify the results of the previous section using the Kullback-Leibler distance method introduced in [12]. This gives a lower limit on the number of events required to discriminate between any two of the spin allocations at a given level of confidence. These lower limits do not include background or detector effects as these will vary between experiments and we wish to remain general. They do provide a handle on the feasibility of distinguishing two particular curves. This analysis is applied to the observable processes individually, and then combined. The conclusions are in section 5 before the more lengthy formulae, which are in the appendix.

## 2. Spin assignments

We will consider the decay of a heavy colour-triplet scalar or fermion  $C$  of the form  $C \rightarrow B \rightarrow q, B \rightarrow A \rightarrow W \rightarrow \ell \nu$  (figure 1), where  $\ell = e, \mu$ . Chains like this can occur in SUSY, UED or the Littlest Higgs model with T-parity.

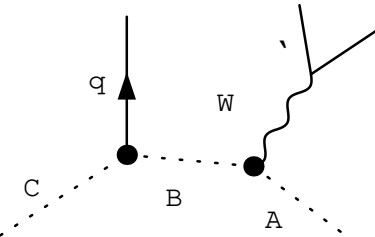


Figure 1: The decay chain under consideration.

We will assume that particle  $A$  is a stable or long-lived heavy massive new particle and that the masses of the new heavy particles  $A, B$  and  $C$  have all been measured. All possible spin configurations are listed in Table 1, together with the labels which will be used in the rest of the paper.

The SFF chain corresponds to SUSY spin assignments while FVV corresponds to the spin assignments in a UED model, or a Littlest Higgs model with T-parity [15]. The UED

Label	C	B	A
SFF	Scalar	Ferm ion	Ferm ion
FSS	Ferm ion	Scalar	Scalar
FSV	Ferm ion	Scalar	Vector
FVS	Ferm ion	Vector	Scalar
FVV	Ferm ion	Vector	Vector

Table 1: Possible spin configurations in the decay chain (figure 1).

masses derived from [16] do not allow a decay chain of this form to proceed for values of the compactification radius accessible at the LHC, however, these were calculated under the assumption that the orbifold boundary kinetic terms vanish at the cut-off scale. This is not necessarily the case and for different values of these parameters it is possible that the decay chain would still proceed.

It is necessary to make some assumptions about the structure of the vertices in the chains, except for the SFF chain where these are well-determined in the MSSM. We are not concerned with overall numerical factors as the distributions are normalized to integrate to 1. When we consider the FSS, FSV, FVS and FVV chains, the B-W-A vertex structure is uniquely determined. For example in the FSV and FVS chains it is of the form  $g_{\mu\nu}^{\alpha\beta}$ , where  $\mu$  is the index corresponding to the W and  $\nu$  is the index corresponding to the other vector particle (A in FSV or B in FVS).

However, the structure of the C-q-B vertex is not so well determined in these chains and in principle contains a factor of  $(1 + a_5)$  where  $a_5$  is an undetermined constant. In the massless quark limit, the final distributions are in fact independent of this factor  $a_5$  for the FSS and FSV chains, but this is not the case for FVS and FVV. For these chains, where necessary, the factor has been taken to be 1, thereby forcing the quark to be left-handed. This value is justified because most models beyond the standard model have two excitations for each fermion | one coupling to the left-handed fermion and one coupling to the right. It is usually the one associated with the left-handed fermion which undergoes decays of the type in figure 1 (especially for the light quarks we consider where the mixing is small). In particular, the FVV chain has the spin structure found in UED where this is the case.

### 3. Spin correlations

In the chain, there are only two observable emitted particles, the quark and the lepton. This gives one observable invariant mass-squared:  $m_{q\ell}^2 = (p_q + p_\ell)^2$ . We define the angle  $\theta$  to be the angle between the quark and A in the rest frame of B, and  $\phi$  to be the angle between the lepton and A in the rest frame of the W. We then define  $\psi$  to be the angle between these two planes. Then,

$$m_{q\ell}^2 = \frac{1}{4X} m_B^2 (1 - X) (1 + Y - Z) (1 - \cos \theta \cos \phi) + \frac{p_\ell}{(1 + Y - Z)^2} \frac{4Y}{4Y} (\cos \theta \sin \phi) \frac{p_q}{2Y} \sin \theta \sin \phi \cos \psi; \quad (3.1)$$

where the mass-squared ratios  $X; Y; Z$  are  $X = m_B^2/m_C^2$ ,  $Y = m_W^2/m_B^2$  and  $Z = m_A^2/m_B^2$ . These must satisfy  $\frac{Y}{X} + \frac{Z}{X} \leq 1$  by energy conservation and so the quantity in the square root is always non-negative. The maximum value of  $m_q^2$  is  $\frac{1}{2X}m_B^2(1-X)((1+Y-Z)^2 - 4Y)$  which occurs when  $(X; Y; Z) = (0; 1; 1)$ .

In order to keep a manageable expression, we define the scaled invariant mass as

$$m_q^2 = \frac{4X}{m_B^2(1-X)}m_q^2; \quad (3.2)$$

which lies in the interval  $0; 2((1+Y-Z)^2 - 4Y)$ .

The analytical expressions valid for any particle masses are discussed in appendix A, however, in order to plot the functions we must choose values for the masses of A; B and C. If we consider this chain in a SUSY scenario, we have the particle assignments given in table 2. The masses given are those at the Snowmass Benchmark points, SPS 1a, SPS 2 and SPS 9 [17]. SPS 1a and SPS 2 were chosen as the points with the biggest difference in their spectrum, while the AMSB point, SPS 9, was chosen as an example of a heavier chargino which allows for a greater difference between Y and Z.

	C $e_L$	B $e_2$	A $e_1^0$
SPS 1a	537	378	96
SPS 2	1533	269	79
SPS 9	1237	876	175

Table 2: The mass spectra (in GeV) considered in this paper.

The spin correlations in the chain where the quark partner decays through a  $W^+$  has different spin correlations to that in which the quark partner decays through a  $W^-$ , so we have two processes to consider:

Process 1:  $f q, W^- g = f u, W^- g$  or  $f u, W^+ g$

Process 2:  $f q, W^- g = f d, W^+ g$  or  $f d, W^- g$ .

Here u stands for either an up or a charm quark and d stands for a down or a strange quark. We do not include bottom and top quarks since b and t final states should be distinguishable from those due to the lighter quarks. We may then work in the massless approximation. For the FSS chain, processes 1 and 2 give the same distribution as the  $W$  boson is produced with longitudinal polarisation.

Figure 2 shows the invariant mass-squared distributions for both processes for the five spin assignments given in Table 1, for the SPS 1a mass spectrum. Here, the distributions are plotted as  $dP = dm$  throughout, as opposed to  $dP = dm^2$  as was done in [12], as the phase space is not flat in any such simple mapping of the invariant mass. The phase space curve (the case where all particles are treated as spinless) also depends on the masses in the chain, and so is indicated on the  $dP_1 = dm$  plot for each mass spectrum (marked No Spin). Figures 3 and 4 show the same distributions for the five spin assignments, for the SPS 2

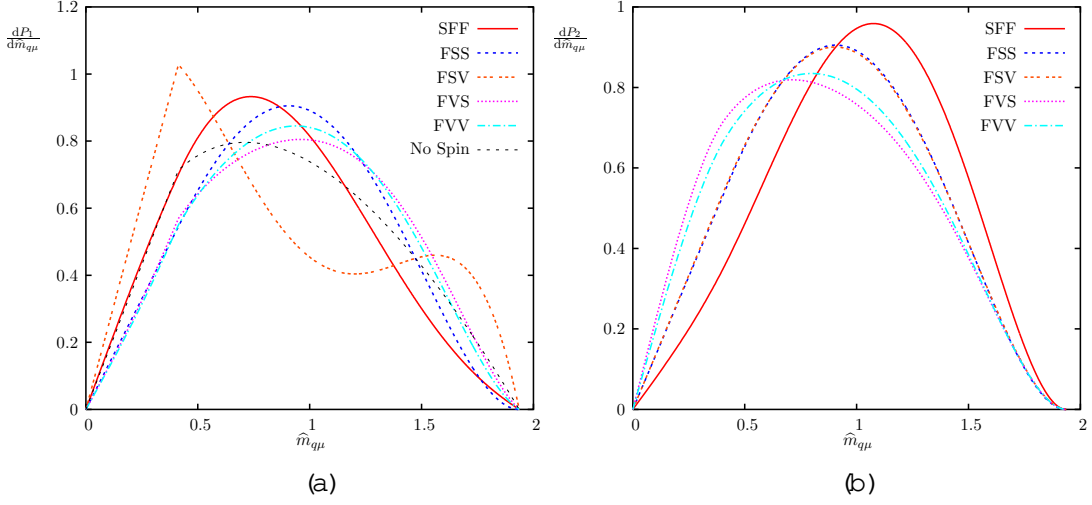


Figure 2: Invariant mass distributions for SPS 1a: (a) Process 1 and (b) Process 2.

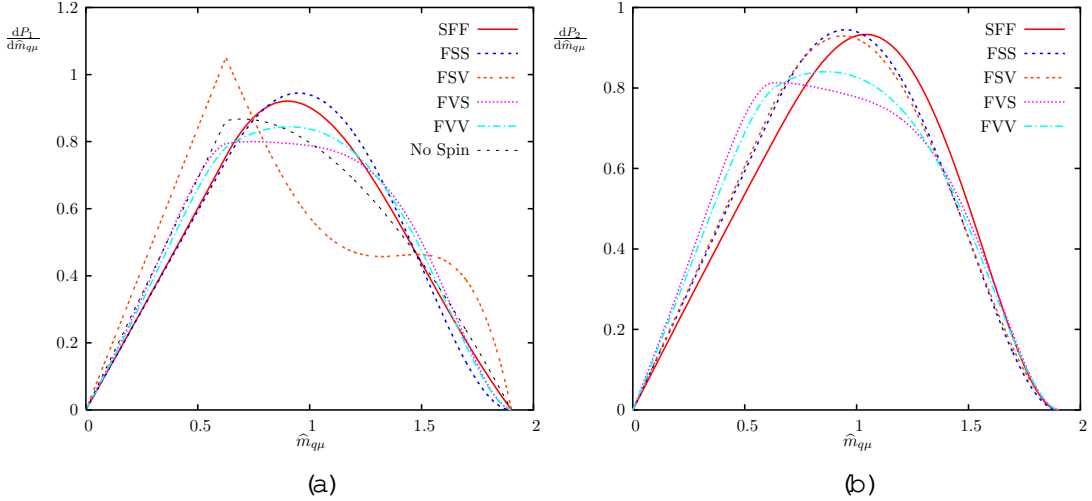


Figure 3: Invariant mass distributions for SPS 2: (a) Process 1 and (b) Process 2.

and SPS 9 mass spectra.

For all 3 mass spectra, the most distinctive curve is the FSV Process 1 curve. While the other curves have one peak just before  $m = 1$  for both processes, the FSV curve for Process 1 has a local minimum there and peaks instead at low and high values of  $m$ . However, in process 2, the FSV curve blends in with the others (particularly FSS). For SPS 1a and SPS 9, the SFF curve peaks slightly to the left (right) of the others in Process 1 (2).

From these curves for processes 1 and 2, we can construct the distribution of processes through a  $W^-$  and the distribution of processes through a  $W^+$ , which are the distributions which would actually be observed. If an  $^-$  is observed, the chain must have started with the partner of either a down-type quark, or an up-type antiquark. We denote  $r_d = 1 - r_u$

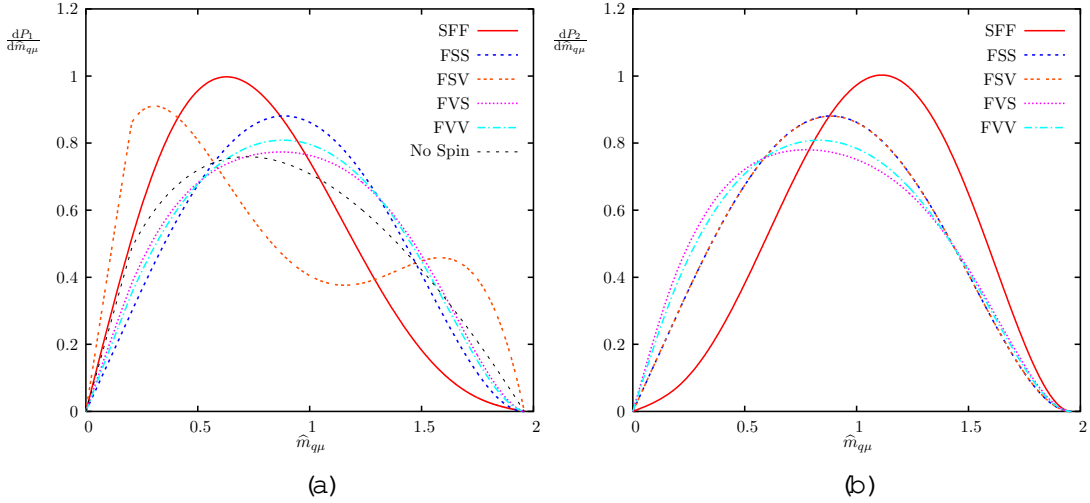


Figure 4: Invariant mass distributions for SPS 9: (a) Process 1 and (b) Process 2.

to be the fraction of chains with an ‘- which begin with the partner of a down-type quark. Similarly, we define  $r_u = 1 - r_d$  to be the fraction of chains with an ‘+ which begin with the partner of an up-type quark. The  $q^\pm$  distributions,  $dP/dm^\pm$ , are given by:

$$\begin{aligned} \frac{dP}{dm^\pm} &= r_d \frac{dP_1}{dm^\pm} + r_u \frac{dP_2}{dm^\pm} \\ \frac{dP_+}{dm^\pm} &= r_u \frac{dP_2}{dm^\pm} + r_d \frac{dP_1}{dm^\pm}; \end{aligned} \quad (3.3)$$

No distinction between flavours of quarks was required in the earlier studies [3, 5, 7, 12] of the cascade decay of a quark partner; in these the quark partner decayed straight into a quark and a neutral particle. No charge information of the original quark was transmitted to the rest of the chain making the results flavour independent.

Running Herwig [18, 19, 20] gives the values of the fractions in table 3 for the SUSY scenarios. These values are model-dependent, but represent a rather wide range of possibilities. We see that at SPS 9, the effect of having more up quarks than down quarks in the proton is dwarfed by the latter’s larger branching ratio to a chargino. This is caused by the large value of the MSSM parameter  $\tan\beta$  enhancing the effect of large  $\tan\beta$  in the chargino mixing matrices. The resulting plots are shown in figures 5 { 7.

Spectrum	$r_d$	$r_u$	$r_u$	$r_d$
SPS 1a	0.860	0.140	0.469	0.531
SPS 2	0.900	0.100	0.911	0.089
SPS 9	0.998	0.002	0.072	0.928

Table 3: Numerical calculation of fractions using Herwig.

We see that in these observable plots, the distinctive shape of the FSV curve is still evident in the  $dP/dm^\pm$  plots (and also in the SPS 9  $dP_+/dm^\pm$  plot due to the large value

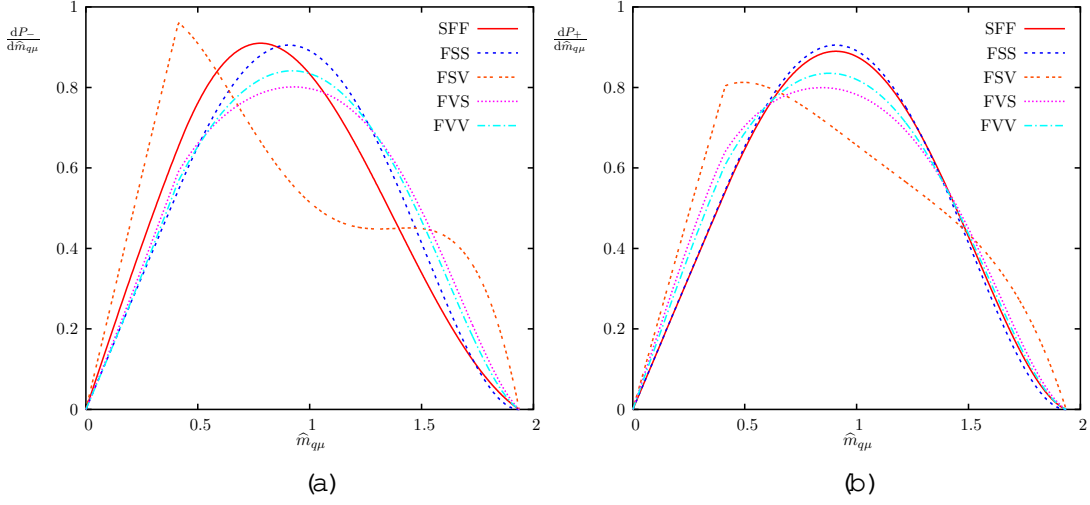


Figure 5: Observable invariant mass distributions for SPS 1a: (a)  $P_-$  and (b)  $P_+$ .

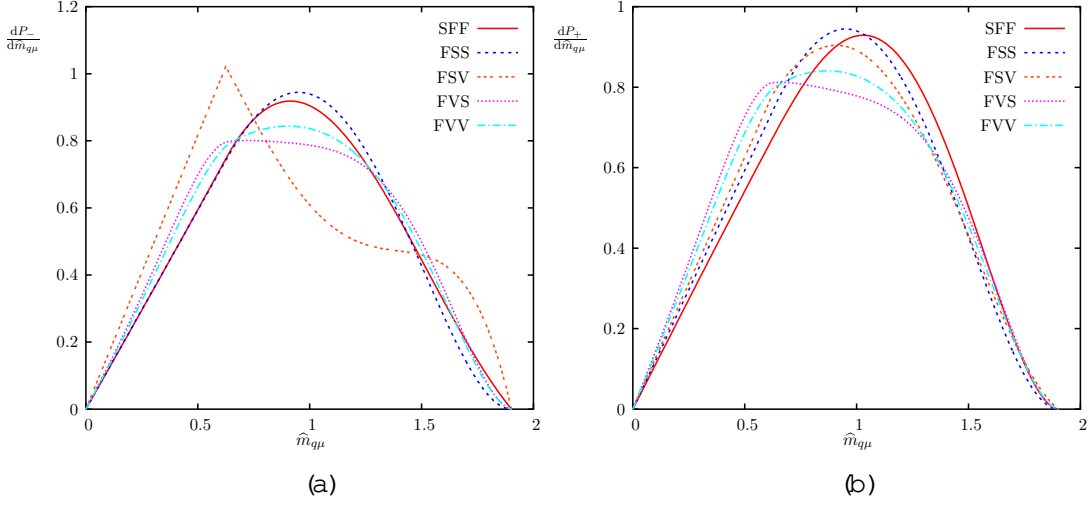


Figure 6: Observable invariant mass distributions for SPS 2: (a)  $P_-$  and (b)  $P_+$ .

of  $r_d^+$ ). In fact at SPS 9, the plots are nearly identical as seen in the asymmetry plot (figure 9). We can be most hopeful about being able to distinguish these curves at the mass point SPS 9, however, the  $P_-$  distributions for all the mass spectra would be useful.

We combine the information from both chains together by forming the asymmetry of the normalized distributions given by

$$A = \frac{\frac{dP}{d\mathbf{p}^2} - \frac{dP_+}{d\mathbf{p}^2}}{\frac{dP}{d\mathbf{p}^2} + \frac{dP_+}{d\mathbf{p}^2}} : \quad (3.4)$$

The resulting plots are given in figures 8 and 9.

The asymmetry plot for SPS 1a (figure 8a) shows striking difference in the behaviour of all the curves, except perhaps between FVS and FVV. With a 10% level of asymmetry

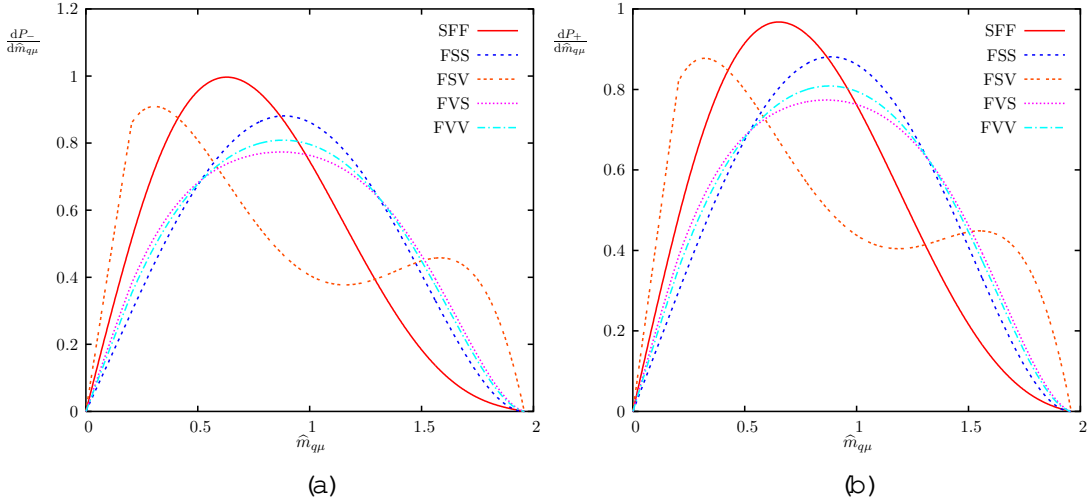


Figure 7: Observable invariant mass distributions for SPS 9: (a)  $P_-$  and (b)  $P_+$ .

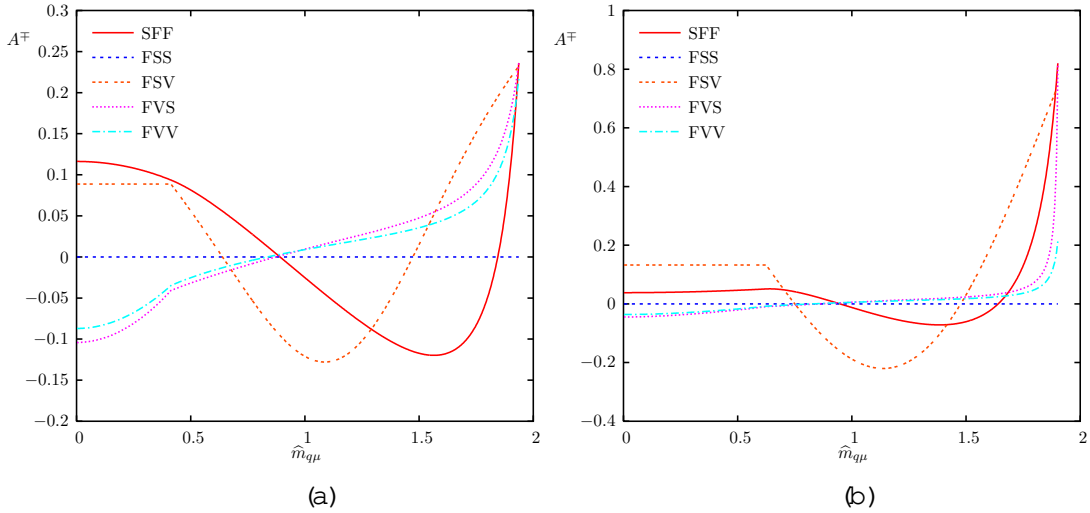


Figure 8: Asymmetry plots for (a) SPS 1a and (b) SPS 2.

at different values of  $\hat{m}$ , we can be optimistic about distinguishing the FSV curve and the SFF curve. Equally if we observed zero asymmetry for all values of  $\hat{m}$  we could be confident that the chain was FSS.

In the asymmetry plot for SPS 2 (Figure 8b), it is unlikely that we would be able to distinguish the FVS and FVV curves from the FSS line of zero asymmetry. The differences at high  $\hat{m}$  would be difficult to use as this is where experimental statistics are usually much worse. However, we could distinguish the FSV line as it shows an asymmetry of 20%. It would be harder to distinguish the SFF line with its peak at just below 10%, but with enough statistics it may be possible.

The asymmetry plot for SPS 9 (Figure 9) shows low levels of asymmetry for all the

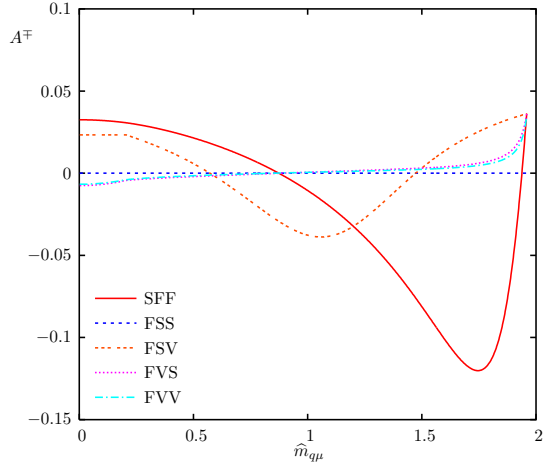


Figure 9: A symmetry plot for SPS 9.

curves, with the exception of the SFF curve. Its peak of over 10% asymmetry gives grounds for optimism that it could be picked out. While, the other curves may be difficult to split in this plot, this was the case where they were easier to separate on the basis of the distribution curves (figure 7).

#### 4. Model discrimination

Here we apply the Kullback-Leibler distance [21] described and discussed in [12]. We recall that it was defined there as

$$K L(T;S) = \int_m \log \frac{p(m|T)}{p(m|S)} p(m|T) dm : \quad (4.1)$$

The minimum bound on the number of events,  $N$ , needed such that distribution  $T$  is  $R$  times more likely than distribution  $S$ , assuming that  $T$  is the true distribution is given in the limit  $N \rightarrow 1$  as

$$N = \frac{\log R + \log \frac{p(S)}{p(T)}}{K L(T;S)} \quad (4.2)$$

where  $p(S)$  and  $p(T)$  are the prior probabilities of each distribution. We must make an assumption about the true distribution as we must generate our data points for comparison from a particular distribution. This will not be the case when we have real data. We include the factor  $\log(p(S) = p(T))$  for completeness, however, we will set it to zero in our analysis. This is equivalent to assuming all distributions to be equally likely before we look at the data. Also, as pointed out in [12], the result is invariant under isomorphism  $f(m)$ , so the result would be unaffected if we had calculated with  $m^2$  for example, instead of  $m$ .

The value  $N$  is an absolute lower bound on the required number of events. Once background and detector effects are included these will rise considerably, however, these effects vary from experiment to experiment and hence it is useful to have a universal lower bound.

The results for the observable  $P^-$  distributions at SPS 1a (figure 5) are given in table 4. The corresponding results for the curves at SPS 2 (figure 6) and SPS 9 (figure 7) are shown in tables 5 and 6.

(a)	SFF	FSS	FSV	FVS	FVV		(b)	SFF	FSS	FSV	FVS	FVV
SFF	1	697	87	367	468		SFF	1	6728	175	1087	2801
FSS	712	1	62	687	1481		FSS	7728	1	151	765	1689
FSV	76	53	1	91	75		FSV	159	127	1	380	254
FVS	339	591	96	1	5640		FVS	1052	713	419	1	6741
FVV	448	1298	80	5783	1		FVV	2734	1590	284	6837	1

Table 4: Number of events needed, with SPS 1a masses, to disfavour the column model with respect to the row model by a factor of 1/1000, assuming the data to come from the row model, for (a)  $dP^- = d\ln$  and (b)  $dP_+ = d\ln$ .

(a)	SFF	FSS	FSV	FVS	FVV		(b)	SFF	FSS	FSV	FVS	FVV
SFF	1	1220	125	1007	2166		SFF	1	1484	1064	425	649
FSS	1608	1	89	638	1292		FSS	1531	1	2909	569	1106
FSV	121	75	1	155	130		FSV	1055	2549	1	1128	3267
FVS	1027	619	177	1	6530		FVS	409	559	1131	1	6365
FVV	2267	1240	146	6537	1		FVV	630	1081	3280	6358	1

Table 5: As in table 4 for the SPS 2 mass spectrum, for (a)  $dP^- = d\ln$  and (b)  $dP_+ = d\ln$ .

(a)	SFF	FSS	FSV	FVS	FVV		(b)	SFF	FSS	FSV	FVS	FVV
SFF	1	90	41	85	87		SFF	1	123	48	116	121
FSS	83	1	36	790	1686		FSS	117	1	42	791	1686
FSV	28	31	1	49	42		FSV	34	35	1	58	49
FVS	69	742	54	1	7451		FVS	98	746	65	1	7529
FVV	73	1605	47	7555	1		FVV	105	1609	56	7632	1

Table 6: As in table 4 for the SPS 9 mass spectrum, for (a)  $dP^- = d\ln$  and (b)  $dP_+ = d\ln$ .

The lower numbers in the SPS 9 tables reflect the original impression from the graphs that the curves are easier to separate at this point than at SPS 1a or 2. The values for SFF and FSV are particularly encouraging: either around or significantly below 100. These will of course be degraded in an experimental situation but give us reason to be optimistic. We see in all the tables that the highest number of events are required to separate FVS and FVV. This is no surprise from the plots.

The numbers in tables 4 - 6 treat the  $W^+$  and  $W^-$  chains individually, however, we can reasonably expect that if one is observed, both will be. The relative numbers of the two chains again depend on the masses in the chain. With experimental data these values would be known, but here we rely on the values from Herwig. The results are shown in table 7, where the fraction of  $W^-$  chains which included a  $W^+$  is denoted  $f$ .

Spectrum	$f_+$	$f$
SPS 1a	0.57	0.43
SPS 2	0.68	0.32
SPS 9	0.67	0.33

Table 7: Fractions,  $f$ , of total number of  $W^-$  chains which include a  $W^+$  for each mass spectrum.

When we consider both sets of data at once, equation (4.1) is generalised to

$$\begin{aligned}
 KL(T;S) &= \sum_m \log \frac{p(m^+ \bar{T}^+)}{p(m^+ \bar{S}^+)} p(m^+ \bar{T}^+) + \log \frac{p(m^- \bar{T}^-)}{p(m^- \bar{S}^-)} p(m^- \bar{T}^-) dm \\
 &= KL^+(T;S) + KL^-(T;S) \tag{4.3}
 \end{aligned}$$

where  $p(m^- \bar{T}^-) = f^- p(m^- \bar{S}^-)$ . This gives the values of  $N$  shown in tables 8 and 9.

(a)		SFF	FSS	FSV	FVS	FVV	(b)		SFF	FSS	FSV	FVS	FVV
SFF	1	1425	122	590	891		SFF	1	1388	312	521	837	
FSS	1476	1	93	730	1593		FSS	1554	1	261	590	1160	
FSV	108	79	1	161	125		FSV	304	220	1	375	375	
FVS	552	655	171	1	6219		FVS	507	577	415	1	6416	
FVV	855	1450	136	6340	1		FVV	819	1127	417	6415	1	

Table 8: Total number of  $W^+$  and  $W^-$  events needed to disfavour the column model with respect to the row model by factor of 1/1000, assuming data to come from the row model at (a) SPS 1a and (b) SPS 2.

	SFF	FSS	FSV	FVS	FVV
SFF	1	110	46	103	107
FSS	103	1	40	791	1686
FSV	32	34	1	55	47
FVS	86	745	61	1	7503
FVV	92	1607	53	7606	1

Table 9: As in table 8, at the SPS 9 mass spectrum.

In order to illustrate how these numbers show an improvement over treating the distributions separately, we consider the specific values of the (SFF,FVS) entry at SPS 1a. For the  $P^-$  distribution alone it was 367, while for  $P_+$  alone it was 1087. For this mass spectrum, close to half (43%) of the chains have a  $W^-$ . This means that looking at the whole sample, for every  $W^-$  event there is at least one  $W^+$  event. If the  $W^+$  events contributed no discriminatory information (that is if  $p(m^+ \bar{S}^F) = p(m^+ \bar{V}^F)$  for all  $m^+$ ), then we would expect to need about  $1 = 0.43 = 2.3$  times the number of  $W^-$  events alone, 844. However, as the  $W^+$  events do contribute to distinguishing the two models, we find that only 590 events in total are required.

Equation (4.2) shows that when the prior probabilities of the models are equal (i.e.  $p(S) = p(T)$  as we have used) the number of events  $N_1$  calculated for a discrimination level

$R = R_1$  is related to the number of events  $N_2$  calculated with  $R = R_2$  by a multiplicative factor. For example, to obtain the results for  $R = 20$  (which corresponds to a 95% confidence level), the numbers in tables 4 & 9 should be multiplied by  $\log(20) = \log(1000) = 0.43$ .

## 5. Conclusions

The spin correlations in the decay of a quark partner via a  $W$  boson, as exhibited in the invariant mass distributions of the quark and lepton, have been studied for three distinct SUSY-inspired mass spectra (SPS points 1a, 2 and 9). We have considered the 5 possible spin assignments in the chain and studied the extent to which they can be distinguished. The observable invariant mass distributions were constructed where we found that we could be particularly optimistic at SPS 9. The distributions at the other points (particularly  $dP = d\theta$ ) could also be useful. The curve for the FSV chain stands out in form from the other curves.

The asymmetry formed from these plots proved to be very useful, particularly at SPS 1a where it was harder to distinguish the spin assignments on the strength of their distributions alone. At SPS 9, the asymmetry plot could clearly distinguish the SFF curve (which corresponds to SUSY) from the others while the  $P$  distributions were more useful to distinguish among the others.

The results were quantified using the Kullback-Leibler distance to give a lower bound on the number of events required to distinguish the spin assignments at a given level of certainty. This was applied to the distributions individually, and then to them combined. These provide a guide to how useful particular channels would be in a study like this.

The study of this decay mode of a quark partner is therefore a potentially powerful tool to extract the spin assignment of the new particles. The combination of information from observed distributions and their asymmetry makes this chain even more useful.

## Acknowledgements

I thank members of the Cambridge Supersymmetry Working Group for helpful discussions while this work progressed. I am particularly grateful to Bryan Webber for constructive comments, numerical checks and useful discussions throughout. I also thank Jeppe Andersen for technical assistance and Ben Allanach for clearing up some points and commenting on a draft.

## A. Analytical formulae

This section contains the formulae for the distributions plotted in section 3 (with the exception of FVV, see below). They are expressed in terms of two constants  $k_1$  and  $k_2$  which are functions of the mass ratios described in section 3:

$$k_1 = 1 + Y \quad Z \quad \text{and} \quad k_2 = \frac{q}{k_1^2 - 4Y}; \quad (A.1)$$

such that  $k_1 > k_2 > 0$ . Then equations (3.1) and (3.2) give

$$\frac{dP}{d\mathbf{p}_q^2} = k_1(1 - \cos \theta) + k_2(\cos \theta - \cos \phi) - \frac{p}{2Y} \sin \theta \sin \phi \cos \phi \quad (A.2)$$

with maximum  $2(k_1 + k_2)$ . We define the shorthands  $k_{12} = k_1 - k_2$  and  $\mathbf{p} = \mathbf{p}_q$ .

SFF

In the MSSM, the structure of the  $B\bar{W}A$  vertex is  $1 + \dots + 5$  where  $\dots$  is defined by the parameters of the model. As this varies at each mass point, it is left explicitly in the equations below. Table 10 lists the values of  $\dots$  at the particular points studied in this paper.

Mass Spectrum	SPS 1a	SPS 2	SPS 9
	0.5083	0.3875	0.8155

Table 10: Numerical values of the parameter  $\dots$  for the different mass spectra studied in the text.

$$\frac{dP_1}{d\mathbf{p}^2} = \frac{3\mathbf{p}}{32k_2((1 + \dots)^2(k_1^2 + 2Y - 3k_1Y) - 6Y \frac{p}{Z}(1 - \dots^2))} \quad (A.3)$$

$$\begin{aligned} & \frac{16}{8} k_2((1 + \dots)^2 k_1 + 4(1 + \dots)^2 Y \\ & + \mathbf{p}^2(1 + 4 + \dots^2 + (1 + \dots)^2 \frac{p}{Z})) - (2k_1 \mathbf{p}^2 \\ & + (2(1 + \dots)^2(1 + k_1) + (1 + \dots)^2 \mathbf{p}^2)Y) \log \frac{k_1 + k_2}{k_1 - k_2} \end{aligned}$$

$$0 \quad \mathbf{p}^2 \quad 2k_{12}$$

$$\begin{aligned} & \frac{8k_1^2(1 + \dots)^2 + (1 + \dots)(6 + \dots)\mathbf{p}^4}{8} \\ & + 8k_1((1 + \dots)^2(k_2 + 4Y) + \mathbf{p}^2(2 + \dots(2 + (2 + \frac{p}{Z})) + \frac{p}{Z})) \\ & + 8\mathbf{p}^2(2(1 + \dots)^2 Y + k_2(1 + 4 + \dots^2 + (1 + \dots)^2 \frac{p}{Z})) \\ & + 16Y((1 + \dots)^2(5 + 2k_2) - 4(1 + \dots)^2 \frac{p}{Z}) - 16(2k_1 \mathbf{p}^2 \\ & + (2(1 + \dots)^2(1 + k_1) + (1 + \dots)^2 \mathbf{p}^2)Y) \log \frac{2(k_1 + k_2)}{\mathbf{p}^2} \end{aligned}$$

$$2k_{12} \quad \mathbf{p}^2 \quad 2k_{12}^+$$

$$\frac{dP_2}{d\mathbf{p}^2} = \frac{3\mathbf{p}}{32k_2((1 + \dots)^2(k_1^2 + 2Y - 3k_1Y) - 6Y \frac{p}{Z}(1 - \dots^2))} \quad (A.4)$$

$$\begin{aligned} & \frac{16}{8} k_2(\mathbf{p}^2 + 4Y - k_1(1 - \dots)^2 + (\mathbf{p}^2(4 + \dots) + 4Y)) \\ & - \mathbf{p}^2 \frac{p}{Z}(1 - \dots^2) - (Y(2 + \mathbf{p}^2 \frac{p}{Z}) + 2(k_1 \mathbf{p}^2 + 2Y)) \\ & + Y(2 + \mathbf{p}^2 + \frac{p}{Z})^2 \log \frac{k_1 + k_2}{k_1 - k_2} \end{aligned}$$

$$0 \quad \mathbf{p}^2 \quad 2k_{12}$$

$$\begin{aligned} & \frac{8k_1^2(1 - \dots)^2 + \mathbf{p}^4(1 + (6 + \dots))}{8} - 16Y(3 + 2k_2 - \frac{p}{4Z}) \\ & + (\frac{10}{8} + (3 + 2k_2 + 4 \frac{p}{Z})) + 8k_1(k_2(1 - \dots)^2 + 2\mathbf{p}^2 \\ & - \mathbf{p}^2 \frac{p}{Z}(1 - \dots^2) - \frac{4Y}{Z}(1 + \dots^2)) - 8\mathbf{p}^2(2Y(1 + \dots)^2 \\ & + k_2(1 + 4 + \dots^2 + \frac{p}{Z}(1 + \dots^2))) + 16(Y(2 + \mathbf{p}^2 \frac{p}{Z}) \\ & + 2(k_1 \mathbf{p}^2 + 2Y)) + Y(2 + \mathbf{p}^2 + \frac{p}{Z})^2 \log \frac{2(k_1 + k_2)}{\mathbf{p}^2} \end{aligned}$$

$$2k_{12} \quad \mathbf{p}^2 \quad 2k_{12}^+$$

F SS

$$\frac{dP_{1;2}}{d\bar{m}} = \frac{3\bar{m}}{2k_2^3} \begin{cases} \frac{8}{8} k_1 k_2 - 2Y \log \frac{k_1 + k_2}{k_1 k_2} & 0 \quad \bar{m}^2 \quad 2k_{12} \\ \frac{1}{16} (6k_1 - 2k_2 - \bar{m}^2) (2(k_1 + k_2) - \bar{m}^2) - 2Y \log \frac{2(k_1 + k_2)}{\bar{m}^2} & 2k_{12} \quad \bar{m}^2 \quad 2k_{12}^+ \end{cases} \quad (A.5)$$

F SV

$$\frac{dP_1}{d\bar{m}} = \frac{3\bar{m}}{2k_2(k_2^2 + 24YZ)} \begin{cases} \frac{8}{8} 2k_1 k_2 + (k_1^2 + 8YZ) \log \frac{k_1 + k_2}{k_1 k_2} & 0 \quad \bar{m}^2 \quad 2k_{12} \\ \frac{1}{8} (2(k_1 + k_2) - \bar{m}^2) (2k_2 - 6k_1 + \bar{m}^2) \\ + 8(k_1^2 + 8YZ) \log \frac{2(k_1 + k_2)}{\bar{m}^2} & 2k_{12} \quad \bar{m}^2 \quad 2k_{12}^+ \end{cases} \quad (A.6)$$

$$\frac{dP_2}{d\bar{m}} = \frac{3\bar{m}}{2k_2(k_2^2 + 12YZ)} \begin{cases} \frac{8}{8} k_1 k_2 + 2Y(2Z - 1) \log \frac{k_1 + k_2}{k_1 k_2} & 0 \quad \bar{m}^2 \quad 2k_{12} \\ \frac{1}{16} (6k_1 - 2k_2 - \bar{m}^2) (2(k_1 + k_2) - \bar{m}^2) \\ + 2Y(2Z - 1) \log \frac{2(k_1 + k_2)}{\bar{m}^2} & 2k_{12} \quad \bar{m}^2 \quad 2k_{12}^+ \end{cases} \quad (A.7)$$

F V S

For the FVS chain the parameter  $a$  represents that in the C-q-B vertex, discussed at the end of section 2.

$$\frac{dP_1}{d\bar{m}} = \frac{9\bar{m} (k_1 + k_2)^2}{8k_2 (1 + a^2) (1 + 2X) (k_1 (k_1 + k_2) - 2Y) (k_1^2 + 8Y)} \begin{cases} \frac{8}{8} 2k_2 (1 + a^2) (k_1 + 6\bar{m}^2) - 4k_2 \bar{m}^2 X (3 + a(2 + 3a)) \\ + (\bar{m}^2 (1 + a^2) (4k_1 + \bar{m}^2) (1 + X)) \\ 4(1 + \bar{a}^2 - 2X(1 + a^2)Y) \log \frac{k_1 + k_2}{k_1 k_2} & 0 \quad \bar{m}^2 \quad 2k_{12} \\ \frac{1}{2} k_2 (2(k_1 + k_2) - \bar{m}^2) (6k_1 k_2 (1 + a^2) (k_2 - 5\bar{m}^2) \\ 8X k_1 k_2 ((1 + a(4 + a))k_2 - 4(1 + \bar{a}^2)\bar{m}^2) \\ + 2k_1^3 (-7(1 + \bar{a}^2) + 4(1 + a(4 + a))X) \\ + k_1^2 (1 + a^2) (16\bar{m}^2 X - 15\bar{m}^2 - 8k_2) \\ + 32Y k_1 (1 + a^2) (-1 + X) + k_2 (k_2 \bar{m}^2 (1 + a^2) (16X - 15) \\ + 8Y (8X(1 + a)^2 - 9(1 + \bar{a}^2))) = (4(k_1 + k_2)^2) \\ + 2k_2 (\bar{m}^2 (1 + a^2) (4k_1 + \bar{m}^2) (1 + X)) \\ 4(1 + \bar{a}^2 - 2(1 + a^2)X)Y \log \frac{2(k_1 + k_2)}{\bar{m}^2} & 2k_{12} \quad \bar{m}^2 \quad 2k_{12}^+ \end{cases} \quad (A.8)$$

$$\begin{aligned}
\frac{dP_2}{d\theta} = & \frac{9i\theta (k_1 + k_2)^2}{8k_2 (1 + a^2) (1 + 2X) (k_1 (k_1 + k_2) - 2Y) (k_1^2 + 8Y)} \\
& \stackrel{8}{\rightsquigarrow} 2k_2 (1 + a^2) (k_1 + 6i\theta^2) - 4X k_2 i\theta^2 (3 + a (3a - 2)) \\
& + (i\theta^2 (1 + a^2) (4k_1 + i\theta^2) (-1 + X) \\
& 4Y (1 + a^2 - 2X (1 - a^2)) \log \frac{k_1 + k_2}{k_1} & 0 & i\theta^2 & 2k_{12} \\
& \stackrel{\frac{1}{8}}{\rightsquigarrow} 2 (2 (k_1 + k_2) - i\theta^2) ((1 + a^2) k_2 (k_1 + k_2) (4k_2 + i\theta^2 (15 - 16X))) & (A.9) \\
& 2 ((1 + a^2) (22k_1 + 26k_2 + 15i\theta^2) \\
& + 16 ((1 - a^2) (k_1 + k_2) + (1 + a^2) i\theta^2 X) Y) = (k_1 + k_2)^2 \\
& + 8 ((1 + a^2) i\theta^2 (4k_1 + i\theta^2) (-1 + X) \\
& 4Y (1 + a^2 - 2X (1 - a^2)) \log \frac{2 (k_1 + k_2)}{i\theta^2} & 2k_{12} & i\theta^2 & 2k_{12}^+
\end{aligned}$$

F V V

The FVV distributions are too long to present here in a manageable way due to the complicated B → W → A vertex. They are available on request from the author.

## References

- [1] T. Appelquist, H.-C. Cheng, and B. A. Dobrescu, "Bounds on universal extra dimensions," *Phys. Rev. D* 64 (2001) 035002, hep-ph/0012100.
- [2] N. Arkani-Hamed, A. G. Cohen, and H. Georgi, "Electroweak symmetry breaking from dimensional deconstruction," *Phys. Lett. B* 513 (2001) 232{240, hep-ph/0105239.
- [3] A. J. Barr, "Using lepton charge asymmetry to investigate the spin of supersymmetric particles at the LHC," *Phys. Lett. B* 596 (2004) 205{212, hep-ph/0405052.
- [4] T. Goto, K. Kawagoe, and M. M. Nojiri, "Study of the slepton non-universality at the CERN Large Hadron Collider," *Phys. Rev. D* 70 (2004) 075016, hep-ph/0406317.
- [5] J. M. Smithe and B. R. Webber, "Distinguishing spins in supersymmetric and universal extra dimension models at the Large Hadron Collider," *JHEP* 10 (2005) 069, hep-ph/0507170.
- [6] M. Battaglia, A. Datta, A. De Roeck, K. Kong, and K. T. Matchev, "Contrasting supersymmetry and universal extra dimensions at the CLIC multi-TeV e+ e- collider," *JHEP* 07 (2005) 033, hep-ph/0502041.
- [7] A. Datta, K. Kong, and K. T. Matchev, "Discrimination of supersymmetry and universal extra dimensions at hadron colliders," *Phys. Rev. D* 72 (2005) 096006, hep-ph/0509246.
- [8] A. Datta, G. L. Kane, and M. Toharia, "Is it SUSY?," hep-ph/0510204.
- [9] A. J. Barr, "Measuring slepton spin at the LHC," *JHEP* 02 (2006) 042, hep-ph/0511115.
- [10] A. Alves, O. Eboli, and T. Pfehn, "It's a gluino," hep-ph/0605067.
- [11] H.-C. Cheng, K. T. Matchev, and M. Schmaltz, "Bosonic supersymmetry? getting fooled at the LHC," *Phys. Rev. D* 66 (2002) 056006, hep-ph/0205314.

[12] C .A thanasiou, C .G .Lester, J.M .Sm illie, and B .R .W ebber, \D istinguishing spins in decay chains at the large hadron collider," JHEP 06 (2006) 082, hep-ph/0605286.

[13] P .M eade and M .R eece, \Top partners at the LHC : Spin and mass measurement," hep-ph/0601124.

[14] L .T .W ang and I .Yavin, \Spin measurements in cascade decays at the LHC ,"  
hep-ph/0605296.

[15] H .C .Cheng and I .Low , \Little hierarchy, little Higgses, and a little symmetry," JHEP 08 (2004) 061, hep-ph/0405243.

[16] H .C .Cheng, K .T .M atchev, and M .Schm altz, \Radiative corrections to Kaluza-Klein masses," Phys. Rev. D 66 (2002) 036005, hep-ph/0204342.

[17] B .C .A llanach et al, \The Snowmass points and slopes: Benchmarks for SUSY searches," Eur. Phys. J. C 25 (2002) 113{123, hep-ph/0202233.

[18] G .C orcella et al, \HERWIG 6: A n event generator for hadron em ission reactions with interfering gluons (including supersymmetric processes)," JHEP 01 (2001) 010,  
hep-ph/0011363.

[19] G .C orcella et al, \HERWIG 6.5 release note," hep-ph/0210213.

[20] S .M oretti, K .O dagiri, P .R ichardson, M .H .Seymour, and B .R .W ebber, \Im plementation of supersymmetric processes in the HERWIG event generator," JHEP 04 (2002) 028,  
hep-ph/0204123.

[21] S .K ullback and R .A .Leibler, \On information and su ciency," Annals of M athematical Statistics 22 (1) (1951) 79{86.